PCCP

Accepted Manuscript

ROYAL SOCIETY OF CHEMISTRY

www.rsc.org/pccp

PCCP

ARTICLE

Phase separation and crystallization in sodium lanthanum phosphate glasses induced by electrochemical substitution of sodium ions with protons

Received 00th January 20xx,
Accepted 00th January 20xx

DOI: 10.1039/x0xx00000x

www.rsc.org/

Keiga Kawaguchi,[a] Takuya Yamaguchi,[b] Takahisa Omata,*[b] Toshiharu Yamashita,[c] Hiroshi Kawazoe,[c] and Junji Nishii[a]

Electrochemical substitution of sodium ions with protons (alkali-proton substitution; APS), and the injection of proton carriers was applied to sodium lanthanum phosphate glasses. A clear and homogeneous material was obtained for a glass of composition $25NaO_{1/2}$-$8LaO_{3/2}$-$66PO_{5/2}$-$1GeO_2$ following APS, with a resulting proton conductivity of 4×10^{-6} Scm^{-1} at 250 °C. The glass underwent phase separation and crystallization at temperatures >255 °C, forming a highly hygroscopic and proton conducting H_3PO_4 phase in addition to LaP_5O_{14} and other unidentified phases. A glass of composition $25NaO_{1/2}$-$8LaO_{3/2}$-$67PO_{5/2}$ underwent phase separation and crystallization during APS, forming both H_3PO_4 and LaP_5O_{14} phases. Sodium lanthanum phosphate glasses are prone to phase separation and crystallization during APS unlike the previously reported $NaO_{1/2}$-WO_3-$NbO_{5/2}$-$LaO_{3/2}$-$PO_{5/2}$ glasses. The phase separation was explained by a reduction in viscosity following APS and the introduction of protons, which exhibit high field strength. Thus, phase separation and crystallization of glasses during APS was difficult to avoid. An approach to suppress phase separation is discussed.

1. Introduction

Intermediate-temperature fuel cells (IT-FCs) working at 250–300 °C have received much attention in recent years because of their better manufacturing cost, energy efficiency and favorable operating conditions when compared with high-temperature solid-oxide or low-temperature polymer-electrolyte fuel cells.[1-3] Solid electrolytes, suitable for use in IT-FCs, are currently being explored extensively.[4-10] Inorganic phosphate glasses show great promise as they can maintain proton carriers at intermediate temperatures.[11] However, most of the protons within these glasses are lost during the production process that requires melting at high temperatures.[12] Therefore, increasing proton carriers in glasses is a major challenge to attain high-proton conductivity in glass electrolytes for use in IT-FCs.

We have developed a technique to inject proton carriers into oxide glasses by the electrochemical substitution of alkali ions in the glass with protons at high temperatures, named alkali-proton substitution (APS).[13,14] The following electrochemical reactions are involved in APS:

$$\tfrac{1}{2}H_2 \text{ (in atmosphere)} \rightarrow H \text{ (in anode)}, \quad (1)$$

$$H \text{ (in anode)} \rightarrow H^+ \text{ (in glass)} + e^- \text{ (to external circuit)}, \quad (2)$$

$$H^+ \text{ (in glass)} + R^+/^-O\text{-P-}O^- \text{ (in glass)} \rightarrow H^+/^-O\text{-P-}O^- \text{ (in glass)} + R^+ \text{ (in glass)}, \quad (3)$$

$$R^+ \text{ (in glass)} + e^- \text{ (from external circuit)} \rightarrow R \text{ (in cathode)}, \quad (4)$$

where R denotes an alkali element. In principle, it is possible to substitute all alkali ions for protons within a glass by applying this technique. Therefore, glasses with extremely high concentrations of proton carriers (10^{21}–10^{22} cm^{-3}) are attainable. These proton concentrations are one to three orders of magnitude higher than those found in glasses fabricated by melting at temperatures >1000 °C.[12-14] In fact, we previously reported the successful injection of proton carriers at a concentration higher than 5×10^{21} cm^{-3} and obtained a pure proton conductor by applying APS to a glass of composition $35NaO_{1/2}$–$1WO_3$–$8NbO_{5/2}$–$5LaO_{3/2}$–$51PO_{5/2}$.[15,16] However, the maximum proton conductivity of the glass after APS was limited to 4.0×10^{-4} Scm^{-1} at 250 °C and displayed low thermal stability, insufficient for use as an electrolyte in IT-FCs. The compositional flexibility of glasses allows the exploration of materials that exhibit high proton mobility and thermal stability.

Sodium lanthanum phosphate glasses are known to be chemically and thermally stable for use in fusion lasers.[17] Herein, we report the application of APS to glasses with nominal compositions (in cationic mol %) of $25NaO_{1/2}$-$8LaO_{3/2}$-$67PO_{5/2}$ (0Ge-glass) and $25NaO_{1/2}$-$8LaO_{3/2}$-$67PO_{5/2}$-$1GeO_2$ (1Ge-glass), and the resulting electrical properties of these materials. Although APS was successful, phase separation and crystallization occurred either during APS or upon post-annealing. The reasons why this occurred in these glasses and

[a] Research Institute for Electronic Science, Hokkaido University, Kita 21 Nishi 10, Kita-ku, Sapporo 001-0021, Japan.
[b] Division of Materials and Manufacturing Science, Graduate School of Engineering, Osaka University, 2-1 Yamada-oka, Suita 565-0871, Japan.
E-mail: omata@mat.eng.osaka-u.ac.jp; Fax: +81-6-6879-7464; Tel: +81-6-6879-7462
[c] Kawazoe Frontier Technologies Corporation, Kuden-cho 931-113, Sakae-ku, Yokohama 247-0014, Japan

an approach to suppress phase separation and crystallization are discussed.

2. Experimantal

2.1. Glass preparation

The sodium lanthanum phosphate glasses 0Ge-glass and 1Ge-glass were prepared by the conventional melt quenching method. The constituent chemicals Na_2CO_3, La_2O_3, H_3PO_4 and GeO_2 were weighed, mixed and then melted in a platinum crucible for 1 h at 1400 °C in air. The molten materials were poured into a carbon mold and annealed at 420 °C for 10 min, then placed in a furnace and allowed to cool down slowly to ambient temperature at −20 °C h^{-1}.

2.2. Alkali-proton substitution (APS)

APS was applied to the as-prepared glasses using an APS apparatus similar to that described in a previous report.[14] Disk-shaped glass plates with a diameter of 18 mm and a thickness of 1 mm were sliced from the cylindrical glass block and both surfaces were then polished. A thin film anode consisting of metallic palladium with a thickness of approximately 0.2 μm was deposited onto one surface of the glass plate by magnetron sputtering. The glass plate was then loaded into a holder made of quartz with the palladium-deposited surface facing upwards. The other face of the glass was positioned to enable contact with a molten tin cathode under a 5% H_2/95% N_2 atmosphere. A DC bias of 20 V was applied between the palladium anode and the molten tin cathode. The APS temperatures and durations for the 0Ge-glass and the 1Ge-glass were 290 °C for 41 h and 310–350 °C for 7.5 h, respectively.

2.3. Characterization

The glass transition (T_g) and deformation (T_d) temperatures were obtained from the thermal expansion curves as measured using a TMA/SS-6000 (SII, Japan). The sodium concentration in the glass was determined using an energy-dispersive X-ray spectrometer (EDX; JED-2300, JEOL, Japan) attached to a scanning electron microscope (SEM; JSM-6335F, JEOL, Japan). The concentration of protons that formed hydroxyl (OH) groups in the glass was determined by the absorbance of the O-H stretching vibration, ν_{OH}, as recorded by a Fourier transform infrared (FTIR) spectrometer (FT-IR6100, JASCO, Japan) with an infrared microscope (IRT-5000, JASCO, Japan). The OH concentration, n_{OH} in cm^{-3}, that corresponds to the proton concentration was calculated from the maximum absorption intensity of ν_{OH} ($\alpha(\nu_{OH})$ in cm^{-1}) using the following equation:[18]

$$n_{OH} = 1.03 \times 10^{19} \times \alpha(\nu_{OH}). \qquad (5)$$

Raman spectra of the glasses were measured using a laser Raman spectrometer (inVia Reflex; Renishaw, UK or NRS-3100; JASCO, Japan) at an excitation wavelength of 532 nm.

The electrical conductivity of the glasses at different temperatures were determined from the impedance spectra recorded using an impedance analyzer (HP4194A) under a dry 5% H_2/95% N_2 atmosphere. Following APS, both surfaces of the glass plate were polished again, giving a ~0.5-mm-thick disk. Subsequently, palladium films were deposited on both surfaces as electrodes. The mean transport number of the protons was calculated from the electromotive force (emf) of a hydrogen concentration cell with the following structure: gas (I), Pd | glass | Pd, gas (II). Gas (I) consisted of 5% H_2/95% N_2 and gas (II) contained a mixture of H_2 and N_2 with H_2 at concentrations ranging from 0.3 to 5%. The experimentally observed emfs were compared to the theoretical values obtained based on the Nernst equation,

$$E = \frac{RT}{2F} \ln\left(\frac{P_{H2}(I)}{P_{H2}(II)}\right) \qquad (6)$$

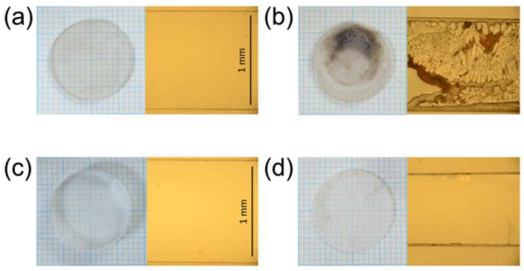

Fig. 1 Photographs (left) and cross-sectional microscope images (right) of glasses. (a) 0Ge-glass before APS, (b) 0Ge-glass after APS, (c) 1Ge-glass before APS and (d) 1Ge-glass after APS.

3. Results

3.1. APS for 0Ge-glass

Photographs and cross-sectional microscope images of the 0Ge-glass before and after APS are shown in Figs. 1 (a) and (b), respectively. Before APS, the glass was stable under atmospheric conditions. However, following APS the glass became partially devitrified and highly hygroscopic. The XRD pattern of the 0Ge-glass following APS (Fig. 2) indicated that both LaP_5O_{14} [19] and other small unidentified phases formed within the sample. The Raman spectrum of 0Ge-glass after APS (Fig. 3 (b)) exhibited sharp peaks that were not present before treatment (Fig. 3 (a)), indicating that the crystallization developed during APS. Additionally, the Raman spectrum after APS exhibited characteristic peaks of P=O stretching modes at 1260–1330 cm^{-1}, $^{-}$O-P-O^{-} symmetric and asymmetric stretching modes at 1100–1230 cm^{-1}, a P-O-P asymmetric stretching mode at ~1050 cm^{-1} and P-O-P symmetric stretching

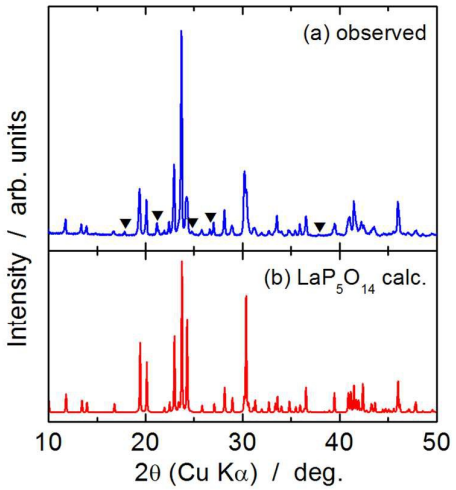

Fig. 2 XRD patterns of (a) 0Ge-glass after APS and (b) LaP_5O_{14} (calculated). Black triangles indicate diffractions from unidentified phase.

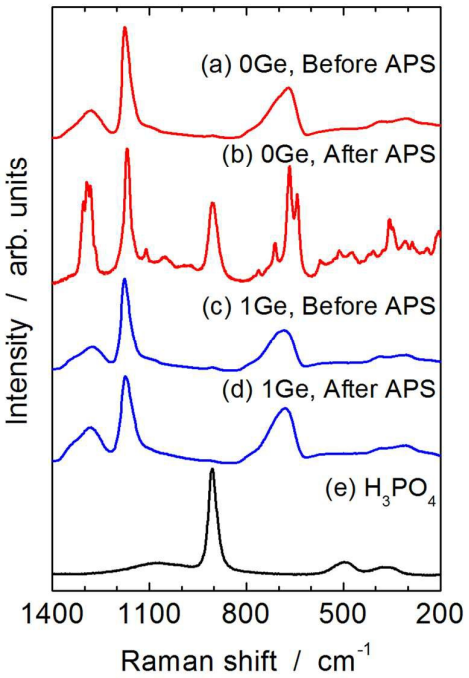

Fig. 3 Raman spectra of 0Ge-glass (a) before and (b) after APS and 1Ge-glass (c) before and (d) after APS. (e) Raman spectrum of H_3PO_4 aqueous solution (85%) for comparison.

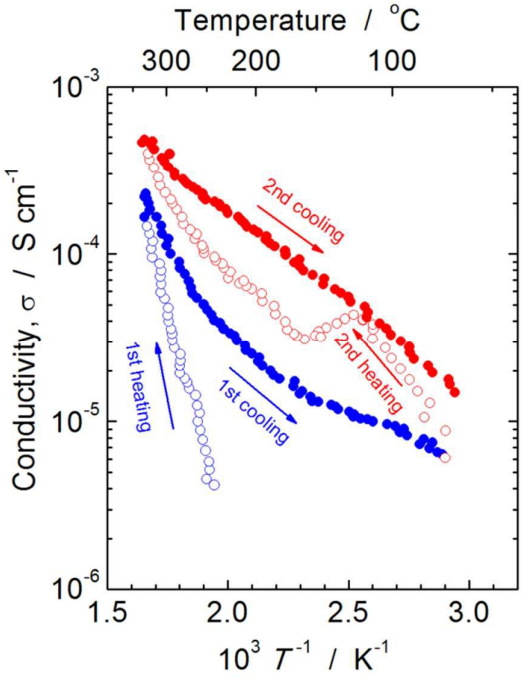

Fig. 5 Arrhenius plots of the total electrical conductivity of 1Ge-glass after APS.

modes at 630–730 cm^{-1} (bending and torsional modes in phosphate framework appear in <500 cm^{-1}, and intensities of those bands are comparatively smaller than those of stretching modes; therefore, we did not discuss about those bands). These peaks were attributed to the presence of LaP_5O_{14} phases.[20] Additionally, an intense peak was observed at ~900 cm^{-1}, which was attributed to the stretching modes of $P(OH)_3$ in phosphoric acid, H_3PO_4 (Fig. 3 (e)).[21] This indicated that the hygroscopic nature of the glass following APS was caused by the formation of H_3PO_4.

3.2. APS for 1Ge-glass

In contrast to the 0Ge-glass, the 1Ge-glass did not crystallize after APS (Figs. 1(c), 1(d), 3(c) and 3(d)), suggesting that the presence of GeO_2 in the glass acted as an effective crystallization-suppressing agent even though only present in very small amounts. The glass after APS was stable in atmospheric condition and did not exhibit hygroscopic nature unlike the 0Ge glass after APS. The concentrations of sodium and OH as a function of distance from the anode for 1Ge-glass before and after APS are shown in Figure 4. The sodium and OH concentrations before APS were 6.3 atomic % (6.2×10^{21} cm^{-3}) (red dotted line) and 6.5×10^{19} cm^{-3} (blue dotted line), respectively. Following APS, the sodium concentration decreased to approximately 2–3 atomic % ($2–3 \times 10^{21}$ cm^{-3}), while the OH concentration increased to approximately 4–5 $\times$ 10^{21} cm^{-3}. The similarity between the values for the decrease in sodium concentration, $3–4 \times 10^{21}$ cm^{-3}, and the increase in OH concentration, $4–5 \times 10^{21} cm^{-3}$, indicated that substitution of sodium ions with protons did indeed occur during APS according to the electrochemical reactions (1)–(4). The Raman spectra of the 1Ge-glass before and after APS (Figs. 3 (c) and (d)) contained peaks consisting of the symmetric stretching mode of P-O-P in phosphate chains ($\nu_{P\text{-}O\text{-}P,sym}(Q^2)$) at 682 cm^{-1}, and $P\text{-}O^-$ symmetric and asymmetric stretching modes at 1176 and 1280 cm^{-3}, characteristic of non-bridging oxygen atoms in phosphate chains ($\nu_{PO2,sym}(Q^2)$ and $\nu_{PO2,asym}(Q^2)$).[22-24] There were no changes observed in these stretching modes after APS, indicating that the glass structure was not affected, unlike the 0Ge-glass and the previously reported $35NaO_{1/2}$-$1WO_3$-$8NbO_{5/2}$-$5LaO_{3/2}$-$51PO_{5/2}$ glass.[25] Therefore, the issues of phase separation and crystallisation encountered with the 0Ge-glass following APS were not present when using the 1Ge-glass.

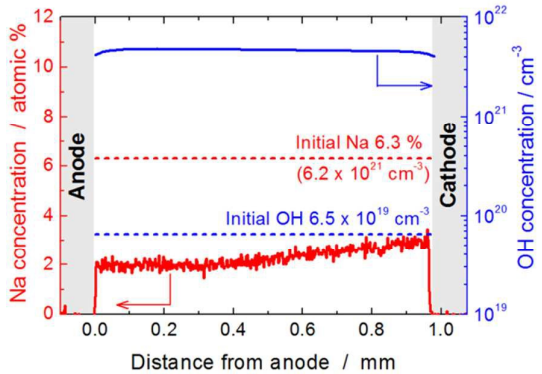

Fig. 4 Concentrations depth profiles of sodium (red line) and OH (blue line) for 1Ge-glass obtained using EDX and FT-IR spectroscopy after APS (18 h). The red and blue dotted lines indicate the sodium and OH concentrations of the glass before APS, respectively.

3.3. Electrical properties of 1Ge-glass after APS

Arrhenius plots of the electrical conductivity of the 1Ge-glass after APS are shown in Fig. 5. The conductivity was measured during two heating and cooling processes. During the first

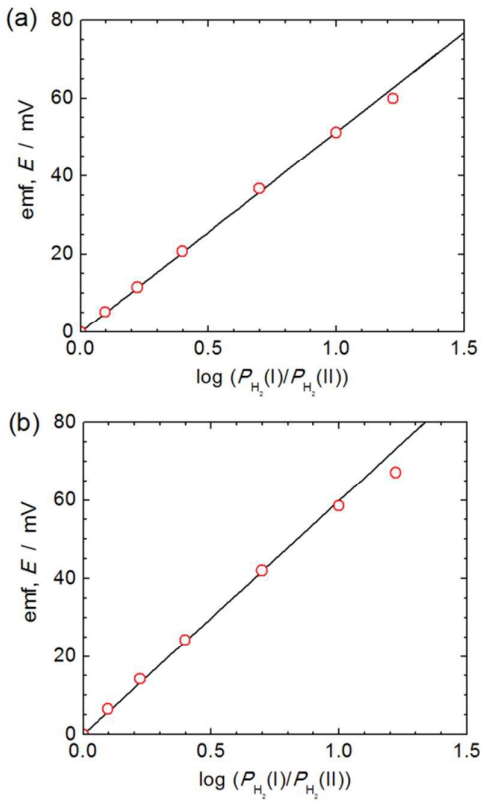

Fig. 6 Emf as a function of a logarithmic P_{H2} ratio in gases (I) and (II) of a hydrogen concentration cell measured at (a) 250 °C and (b) 330 °C. The P_{H2} in gas (I) was fixed as 4.9×10^3 Pa. The theoretical emf values were calculated by the Nernst equation, equation (6), are shown in the figure (black line). Both data were acquired during the 1st heating as indicated in Fig. 5.

heating process, the conductivity increased from 4×10^{-6} Scm^{-1} (240 °C) to 2×10^{-4} Scm^{-1} (330 °C). This yielded an activation energy of 1.14 eV. The emf as a function of the logarithmic P_{H2} ratio of gases (I) and (II) (in a hydrogen concentration cell incorporating APS exposed 1Ge-glass as electrolyte) at 250 and 330 °C are shown in Figs. 6 (a) and (b), respectively. The observed emf increased with the P_{H2} ratio, exhibiting values that were almost identical to the theoretical values calculated using the Nernst equation. This gave a mean proton transport number of one in the glass exposed to the APS process. Thus, following APS the glass was a pure proton conductor in the measured P_{H2} region, although some sodium ions remained in the glass as shown in Fig. 4. These results confirmed that APS is a suitable technique to inject proton carriers in a range of phosphate glasses, considering the composition of 1Ge-glass is quite different from those previously reported.[13-16]

The conductivities observed in the first cooling process were higher than those in the first heating process. Additionally, the activation energy decreased significantly. Similar changes were observed in the successive heating and cooling processes. These observations clearly indicated that the glass changed irreversibly at high temperatures used for the conductivity measurements. When the sample was cooled to ambient temperature after the second cooling cycle, the glass devitrified and became hygroscopic indicating phase separation and crystallization. XRD pattern and Raman spectrum of the 1Ge-glass after APS and post-annealing at 400 °C for 12 h under a

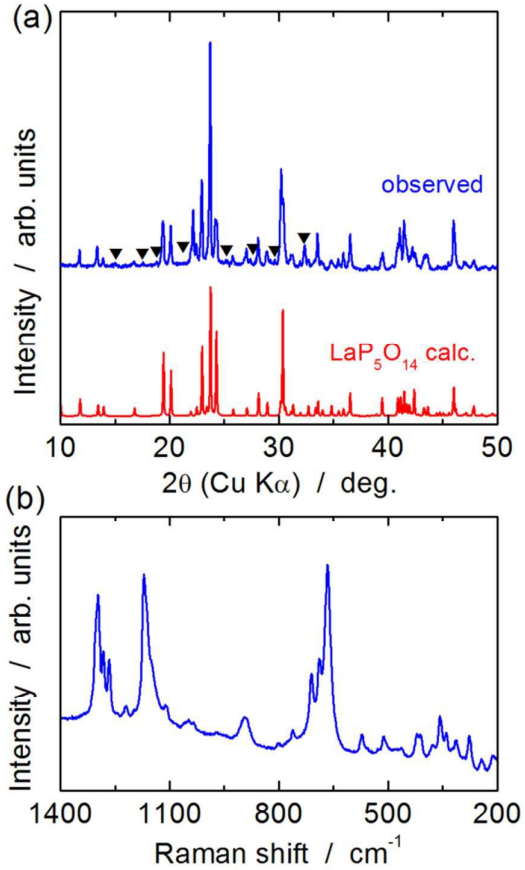

Fig. 7 (a) XRD patterns and (b) Raman spectrum of 1Ge-glass after APS and post annealing at 400 °C for 12 h under a 5%H_2/95N_2 atmosphere. Black triangles in XRD pattern indicate diffractions from unidentified phase.

5%H_2/95%N_2 atmosphere are shown in Fig. 7. These were the same as those of 0Ge-glass following APS (Figs. 2 and 3 (b)). Therefore, it appeared that the 1Ge-glass transformed into a mixture of LaP_5O_{14}, H_3PO_4 and other unidentified crystals after APS.

Phase separation and crystallization of the 1Ge-glass after APS was also evident when examining a plot of the conductivity as a function of time (Fig. 8). The conductivity did not change at temperatures of 200 and 245 °C (6 h holding times at each temperature). However, when the temperature was elevated to 255 °C, the conductivity gradually increased over time. As the temperature was increased further, the rate of conductivity change clearly increased. Finally, the conductivity increased from 2×10^{-4} to 3×10^{-3} Scm^{-1} after 5 h holding time at 290 °C. Thus, phase separation, resulting in a highly conductive phase, developed in 1Ge-glass after APS at temperatures higher than 255 °C. The conductivity of the glass gradually decreased after 65 h at 290 °C. As the holding time was prolonged to 180 h, the conductivity dropped almost three orders of magnitude lower than the maximum value observed at this temperature. Based on the phase separation and crystallization observed in 1Ge-glass after APS and post annealing at 400 °C, the increase in conductivity observed was attributed to the formation of H_3PO_4 phases that are known to

exhibit excellent proton conducting properties, and its subsequent decrease was attributed to vaporization and/or

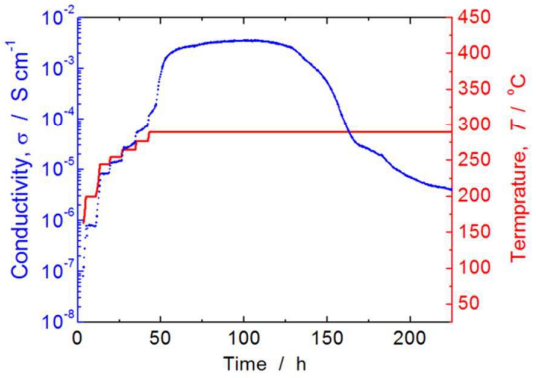

Fig. 8 Change in electrical conductivity as a function of time and temperature for 1Ge-glass after APS.

dehydration of H_3PO_4. The formation of H_3PO_4 phases frequently can be misleading as to the proton conductivity of phosphate materials, as the proton conductivity of H_3PO_4 is significant even at very low concentrations. Ceramic materials prepared using high temperature solid state reactions with unreacted phosphate source materials, are prone to form H_3PO_4 that is not detected by XRD. Therefore, the proton conducting phase must be carefully identified in phosphate materials. The high proton conductivity observed in the 1Ge-glass (3×10^{-3} Scm^{-1} at 290 °C, Fig. 8) was not an intrinsic property of the glass after APS, but was derived from the formation of H_3PO_4 phases.

4. Discussion

The phase separation and crystallization observed in the glasses used in this study can be explained by the protons, injected by APS, binding to oxygen ions and forming OH groups as observed in the infra-red absorption spectrum.[12,13-16,26] These OH groups do not bridge the glass network as the replaced sodium ions did prior to APS. (sodium ions generally have a six-fold coordination to oxygen ions in oxide glasses).[27] Following APS, a previously reported glass of composition $35NaO_{1/2}$-$1WO_3$-$8NbO_{5/2}$-$5LaO_{3/2}$-$51PO_{5/2}$ exhibited a significant decrease in T_g value (200–230 °C lower than that before APS).[16] Consistent with this report, the T_g of the 1Ge-glass decreased from 359 °C to 227 °C after APS (Fig. 9). The APS process for the 0Ge-glass was conducted at 290 °C, lower than its T_g prior to APS (342 °C). However, this temperature should be higher than T_g of the glass after APS, although T_g of the 0Ge-glass after APS was not cleared because of the phase

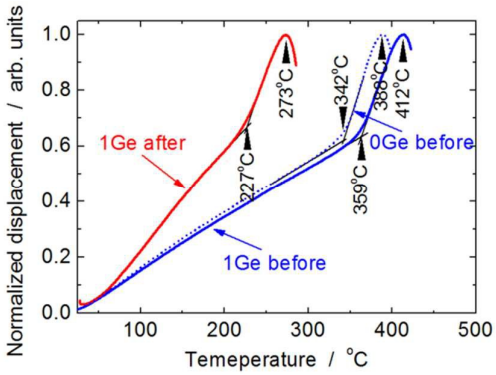

Fig. 9 Thermal expansion curves of 0Ge-glass before APS (blue dotted line) and 1Ge-glass before (blue solid line) and after (red solid line) APS.

separation and crystallization. This induced a decrease in the viscosity as the APS process progressed, which allowed diffusion of ions necessary to cause phase separation and crystallization. This appears to be a major challenge that needs to be controlled to overcome phase separation and crystallization during APS.

Another important factor is the different chemical features of sodium ions and protons. Based on the different phases that appeared in the 0Ge-glass after APS (*i.e.* multi-phases of LaP_5O_{14}, H_3PO_4, unidentified crystals and glass), the crystallization must have occurred accompanying the phase separation. Phase separation in glasses is a well-documented problem and is explained using the ionic field strength of cations, as proposed by Dietzel.[27,28] The field strength is defined by z_+/a^2, where z_+ is the valence of a cation and a is the bond length between a cation and an oxygen ion in an oxide glass. Phase separation in glasses occurs when a cation other than glass former (P^{5+} in the present case) has a large field strength.[29,30] The valence, coordination numbers,[27] ionic radii,[31] bond lengths and field strengths of typical cations in glasses are summarized in Table 1. The field strength of lanthanum ions (0.53) is large when compared with other network-modifying cations used in glasses with field strengths ranging between 0.1 and 0.4.[27] Therefore, lanthanum ions increase the tendency of phase separation. However, the high concentration of sodium ions in the glass before APS, for which the field strength is very small (0.18), decreased the tendency of phase separation. Thus, the 0Ge-glass (with a composition of $25NaO_{1/2}$-$8LaO_{3/2}$-$67PO_{5/2}$) is a highly stable and homogenous glass. During APS, low field strength sodium ions are substituted with high field strength protons (1.06) allowing phase separation to occur as

Table 1 Ionic field strengths of typical cations used in glasses.

Element	Valence	Coordination number	Ionic radius (Å)	Bond length (Å)	Field strength
P	5	4	0.17	1.52	2.16
W	6	6	0.60	1.95	1.58
Ge	4	4	0.39	1.74	1.32
Nb	5	6	0.64	1.99	1.26
Al	3	4	0.39	1.74	0.99
Al	3	6	0.535	1.885	0.84
La	3	6	1.03	2.38	0.53
Ca	2	8	1.12	2.47	0.33
Ba	2	8	1.42	2.77	0.26
Li	1	4	0.59	1.94	0.27
Li	1	6	0.76	2.11	0.22

Na	1	6	1.02	2.37	0.18
H	1	1	−0.38	0.97	1.06

APS progresses. A study in which the sodium ions in a stable soda-lime glass were exchanged for lithium ions (0.22 or 0.27) showed that phase separation and crystallization occurred.[32,33] Therefore, it is quite reasonable to assume that the substitution of sodium ions with protons promotes phase separation in the glasses we have examined.

The conditions used for APS for the 1Ge-glass were almost identical to those used for 0Ge-glass. However, phase separation and crystallization during APS did not occur for 1Ge-glass. Plausibly, the crystallization-suppressing effect of the additional GeO_2 may stem from its excellent network-forming properties in glasses. However, phase separation and crystallization ultimately developed when the glass was left at temperatures higher than its T_g (227 °C) for several hours. This implied that the GeO_2 was acting as a nucleation-suppressing agent.

Although APS is a powerful technique to inject proton carriers into phosphate glasses for the development of a proton conducting electrolyte for use in IT-FCs, it appears difficult to suppress phase separation and crystallization of the glasses because: (i) substitution of sodium ions with protons significantly decreases the T_g; this results in reduced viscosity at high temperatures, eventually promotes ionic diffusion inducing phase separation, (ii) although cations that increase the T_g of the glass can be included, such as La^{3+}, Al^{3+}, Nb^{5+} and W^{6+}, they also increase the tendency of phase separation because they have high field strengths and (iii) substitution of low field strength sodium ions with high field strength protons promotes phase separation. Consequently, there is a trade-off between high proton concentrations and high thermal stability in glasses.

A plausible approach to minimize phase separation after APS involves increasing the number of cation species having high field strength. In these systems, the tendency for phase separation should decrease because the attraction of oxygen ions from cations would compete among the cations. In addition, increase in entropy would be expected to stabilize a homogenous glass state.[29,34] Indeed, there are reports of proton conducting glasses fabricated using APS that contain 3–5 different species of cations with high field strength (such as W^{6+}, Nb^{5+}, La^{3+}, Al^{3+} and Y^{3+}) in addition to P^{5+} ions and protons. The stabilizing effect observed in these glasses after APS was significant.[14-16]

5. Conclusion

In summary, we have applied APS to glasses of composition $25NaO_{1/2}$-$8LaO_{3/2}$-$67PO_{5/2}$ and $25NaO_{1/2}$-$8LaO_{3/2}$-$66PO_{5/2}$-$1GeO_2$ in an attempt to inject proton carriers. The glass of composition $25NaO_{1/2}$-$8LaO_{3/2}$-$66PO_{5/2}$-$1GeO_2$ yielded a clear and homogeneous glass with a high concentration of proton carriers (4×10^{21} cm^{-3}). This glass exhibited pure proton conducting behavior, with an electrical conductivity of 2×10^{-4} Scm^{-1} at 330 °C. However, phase separation and crystallization developed in the glass at this temperature. The glass of composition $25NaO_{1/2}$-$8LaO_{3/2}$-$67PO_{5/2}$ exhibited phase separation and crystallization following APS, resulting both H_3PO_4 and LaP_5O_{14} phases. The observed phase separation was explained by a reduction in viscosity after APS, due to the breaking of bridges within the glass network. Additionally, the introduction of protons, which have high field strength, in place of sodium ions promoted phase separation. Consequently, although APS is a powerful technique to inject proton carriers into phosphate glasses, it is difficult to suppress phase separation and crystallization. To realize high proton conducting glasses for use in IT-FCs, we propose to increase the number of cation species having high field strength. This should suppress the tendency of phase separation because the attraction of oxygen ions from cations would compete among the cations and increase in entropy would be expected to stabilize a homogenous glass state.

Acknowledgements

This work was supported in part by the Advanced Low Carbon Technology Research and Developing Program of the Japan Science and Technology Agency (JST-ALCA).

References

1 D. J. L. Brett, A. Atkinson, N. P. Brandon and S. J. Skinner, *Chem. Soc. Rev*., 2008, **37**, 1568.
2 B. Zhu, *J. Power Sources*, 2001, **93**, 82.
3 J. P. P. Huijsmans, F. P. F. Berkel and G. M. Christie, *J. Power Sources*, 1998, **71**, 07.
4 T. Norby, *Solid State Ionics*, 1999, **125**, 1.
5 E. D. Wachsman and K. T. Lee, *Science*, 2011, **334**, 935.
6 J. Huang, F. Xie, C. Wang and Z. Mao, *Int. J. Hydrogen Energy*, 2012, **37**, 877.
7 E. Fabbri, D. Pergolesi and E. Traversa, *Chem. Soc. Rev.*, 2010, **39**, 4335.
8 E. Fabbri, L. B. D. Pergolesi and E. Traversa, *Adv. Mater.*, 2012, **24**, 195.
9 H. Iwahara, H. Uchida, K. Ono and K. Ogaki, *J. Electrochem. Soc.*, 1988, **135**, 529.
10 D. A. Boysen and S. M. Haile, *Chem. Mater.*, 2003, **15**, 727.
11 Y. Abe, M. Hayashi, T. Iwamoto, H. Sumi, L. L. Hench, *J. Non-Cryst. Solids*, 2005, **351**, 2138.
12 H. Sumi, Y. Nakano, Y. Fujishiro, T. Kasuga, *Solid State Sci.*, 2015, **45**, 5.
13 T. Ishiyama, S. Suzuki, J. Nishii, T. Yamashita, H. Kawazoe and T. Omata, *J. Electrochem. Soc.*, 2013, **160**, E143.
14 T. Ishiyama, S. Suzuki, J. Nishii, T. Yamashita, H. Kawazoe and T. Omata, *Solid State Ionics*, 2014, **262**, 856.
15 T. Ishiyama, J. Nishii, T. Yamashita, H. Kawazoe and T. Omata, *J. Mater. Chem. A*, 2014, **2**, 3940.
16 T. Yamaguchi, T. Ishiyama, K. Sakuragi, J. Nishii, T. Yamashita, H. Kawazoe and T. Omata, *Solid State Ionics*, 2015, **275**, 62.
17 Y. Jiang, S. Jiang and Y. Jiang, *J. Non-Cryst. Solids*, 1989, **112**, 286.
18 Y. Abe and D. E. Clark, *J. Mater. Sci. Lett.*, 1990, **9**, 244.
19 J. Zhu, H. Chen, Y. D. Wang, S. Zhang, W. D. Cheng and H. T. Guan, *Chinese. J. Struct. Chem.*, 2011, **30**, 648.
20 A. Mbarek, G. Chadeyron, D. Avignant, D. Boyer, M. Fourati and D. Zambon, *J. Sol-Gel Sci. Technol.*, 2013, **68**, 193.
21 W. W. Rudolph, *Dalton Trans.*, 2010, **39**, 9642.
22 R. K. Brow, *J. Non-Cryst. Solids*, 2000, **263-264**, 1.
23 R. K. Brow, D. R. Tallant, J. J. Hudgens, S. W. Martin and A. D. Irwin, *J. Non-Cryst. Solids*, 1994, **177**, 221.
24 M. Tatsumisago, Y. Kowada and T. Minami, *Phys. Chem. Glasses*, 1988, **29**, 63.
25 T. Ishiyama, T. Yamaguchi, J. Nishii, T. Yamashita, H. Kawazoe, N. Kuwata, J. Kawamura and T. Omata, *Phys. Chem. Chem. Phys.*, 2015, **17**, 13640.
26 Y. Abe, H. Shimakawa, *J. Non-Cryst. Solids*, 1982, **51**, 357.

27 W. Vogel, *Glass Chemistry second edition*, Springer-Verlag, Berlin, 1994, pp. 45-48.
28 A. Dietzel, Z. *Elektrochem.*, 1942, **48**, 9.
29 W. Vogel, *Glass Chemistry second edition*, Springer-Verlag, Berlin, 1994, pp. 120-122.
30 T. Kokubo, K. Yamashita and M. Tashiro, *Yogyo-Kyokai-Shi*, 1973, **81**, 12.
31 R.D.Shannon, *Acta Cryst.*, 1976, **A32**, 751.
32 F. M. Ernsberger, *Advances in Glass Technology*, Prenum, New York, 1962, pp. 511-524.
33 H. Yunqiu, P. H. Duvigneaud and E. Plumat, *J. Non-Cryst. Solids*, 1991, **127**, 81.
34 Y.-M. Sung, *J. Mater. Res.*, 2002, **17**, 517.